CORRECTIVE SUBREFLECTORS FOR MILLIMETRE AND SUB-MILLIMETRE WAVE APPLICATIONS

Viskum, H.-H.
TICRA
Læderstræde 34
1201 Copenhagen K
Denmark
hhv@ticra.com

van 't Klooster, C.
ESTEC
Keplerlaan 1
2200 AG Noordwijk
The Netherlands
kvtkloos@estec.esa.nl

Zocchi, F.& Binda,P.
Media Lario S.r.l.
Località Pascolo
23842 Bosisio Parini
Italy
fzocchi@media-lario.it

Wagner, R.

Bernhardstr. 43/2
D - 88677 Markdorf
Germany
ru.wagner@t-online.de

Abstract

A mechanically controllable reflector has been manufactured by using an electroformed Nickel shell supported and controlled by 19 actuators. If such a system is used as subreflector in a millimetre-wave antenna system for limb-sounding applications, it is possible to reduce the accuracy requirements to the main reflector and thereby save on overall costs. Instead, the shape of the subreflector is controlled to correct for the thermally induced deformations on the main reflector. The paper describes the method of generating the desired subreflector shape for given distortions, and the experimental model that is used to demonstrate the feasibility of the technique.

Introduction

High-resolution space-borne millimetre and/or sub-millimetre wave radiometers require accurate antennas as instrument sensor. Main reflectors, large in terms of wavelengths, with very demanding surface accuracies are needed, while the antenna system has to satisfy stringent pointing requirements. The antenna pattern performance determines overall instrument performance for a large part.

The cost of a very precise and stable main reflector as well as a dedicated, precise antenna-pointing device can be very high. Consequently, alternatives are of strong interest for such type of antenna applications.

Such an alternative approach is investigated in this paper in which the main reflector is allowed to have some relaxation concerning the surface accuracy over a thermal band, provided the deviations are precisely known. A reconformable subreflector is then used to adapt and correct the deviations of the main reflector.

The correction of the aperture phase front in a reflector antenna by means of a deformable main-, sub- or even additional reflector is not new. Such an approach is already in use in optical or near-infrared telescopes and in a few radio telescope antennas, like for instance the 100 metre Greenbank radio telescope. A correction has also been considered for millimetre and submillimetre wave applications in the 30 meter Pico Veleta radio telescope [1]. The subject was investigated for telecommunication applications in [2], but with emphasis on beam reconfiguration.

Here we consider a reconformable reflector for correction of deviations in the main reflector in a tentative high-resolution radiometer configuration. A reconformable mirror has the potential to be operated in an adaptive mode, assuming that the main reflector surface to be corrected is known, either through measurement (in situ) or through analysis.

For our investigations we have considered the antenna configuration taken from the ADMIRALS mm/sub-mm wave antenna [3]. The latter configuration was investigated in an ESA study for limb-sounder application.

Limb sounding provides atmospheric information about certain chemical elements in vertical sense and so contributes to the knowledge of the distribution of these elements in the atmosphere. Ozone is just one of the targets to be evaluated through measurement of for instance the chlorine spectral line, since chlorine can act as a catalyst in the breakdown process of the ozone.

Antennas needed for such applications have dimensions as given by the ADMIRALS antenna, 2.20 m by 0.8 m, providing a resolution of some 2 to 5 km at about 3000 km distance, when looking from a polar orbiting satellite over the horizon. The pointing requirement is also clear for such an application.

Three possible applications can be noted:

1. A possibility for the relaxation of the surface accuracy requirements for the main reflector. The correction of deviations - if any - with a reconformable subreflector is a way forward. Also an additional reconformable (tertiary) reflector can be used [1].
2. A possibility to correct for pointing errors. High-resolution instruments operating in the sub-millimetre wave regime are demanding in terms of pointing requirements. The space platform may not, or only with difficulty, be

able to provide a stringent pointing capability. A re-conformable reflector assists to point the pattern of the instrument sensor in the direction derived from, for instance, star-sensor information.

3. A possibility to shape or broaden the antenna pattern, as indicated already in the results derived below. For sensors operating from highly elliptical orbits, such a capability can be useful to provide a "zooming" antenna pattern. Such a result might be considered for telecommunication applications when it comes to operating at higher frequencies.

In this paper we will present the results of a detailed investigation of reconformable subreflectors to correct for imperfections in main reflectors for limb sounders as the ADMIRALS antenna above. As an alternative main reflector we propose a reflector made out of a sandwich construction with electroformed Nickel skin as reflecting surface. The configuration has been mechanically analysed for different thermal scenarios, and the subreflector profiles needed to compensate for the distortions are obtained theoretically. It is shown that almost complete restoration of the antenna beam is possible.

An elegant breadboard model of a subreflector has been manufactured with a very thin Nickel skin resting on 19 precision laboratory type actuators. The desired subreflector shape can be set by applying displacements via the actuators, and the resulting surface shape has then been measured. The measured profile is subjected to RF pattern analysis to show the extent to which the nominal shape is restored. While the theoretically perfect restoration is not achieved, it is shown that a very large improvement in the performance is obtained by using the controllable subreflector.

Compensation of main reflector distortions by way of subreflector shaping

The method of compensation is most easily explained by way of example, and to this end we will consider a limb-sounder application for the ADMIRALS experiment (ESA contract [3]). The antenna configuration is the same as for the MASTER instrument described by Jørgensen et al. [4]. The main feature of interest here is the elliptical main reflector with a footprint of 2.2 m by 0.8 m and the subreflector which is approximately 0.16 m in diameter. Both main and subreflectors are shaped using the program DORELA [5], which, based on Geometrical Optics (GO), deforms the surfaces such that the subreflector will efficiently illuminate the elliptical main aperture while the main reflector compensates for the phase error inevitably introduced by the subreflector shaping. A drawing of the geometry is shown in Figure 1 where rays are emanating from the feed and reflected three times before propagating in the main-beam direction. In the present context we will not be concerned with the first of the three reflectors which is only present to provide a more compact optics arrangement.

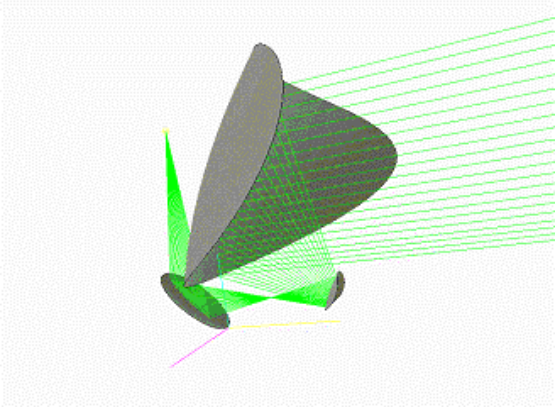

Figure 1. ADMIRALS shaped reflector system

The requirement to the main-reflector surface accuracy is an RMS error of less than 10μm for adequate beam efficiency at 500 GHz, a condition that places severe constraints on the reflector manufacturing and consequently increases the associated costs.

An alternative approach is to manufacture the main reflector as a sandwich construction with a honeycomb Aluminium core and electroformed Nickel skin as reflecting surface. A thorough thermal analysis has been made of such reflector for a number of different thermal load-cases corresponding to different orbital situations for a 600 km polar orbit, revealing significant profile distortions much higher than the specifications.

The most illustrative way of quantifying the thermal distortions is to compare the radiation pattern from the antenna in the nominal stage and after thermal deformations are applied to the main reflector. A representative pattern for the nominal case and a "cold" case (-85 ºC) is shown in Figure 2 for the narrow plane of the beam.

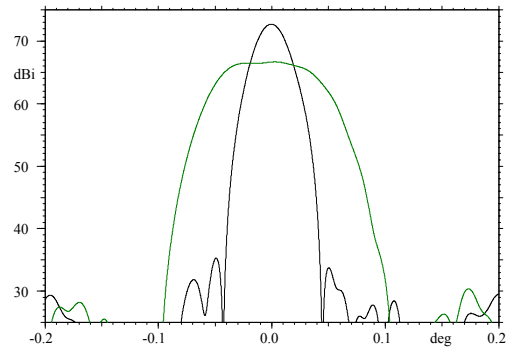

Figure 2. Narrow plane, nominal and cold case.

A significant degradation can be observed from the high-gain narrow spot beam to the degraded and dramatically widened beam, with a gain loss of more than 6 dB. In the orthogonal plane the relative beam widening is less severe, since the nominal beam is already wide in this plane, but the on-axis gain degradation is the same as above.

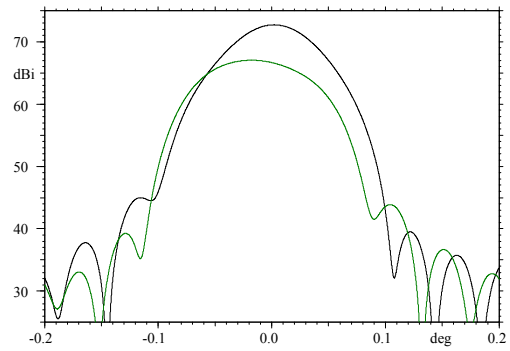

Figure 3. Broad plane, nominal and cold case.

Such performance is of course intolerable in practice. A way to improve is to correct the pattern by adjusting the subreflector to account and compensate for the main-reflector distortions. With an in-orbit controllable subreflector this process can be performed dynamically and programmed to follow the diurnal thermal changes experienced by the main reflector.

The new subreflector profile is derived in the following way:

- expand the distorted main reflector profile in Zernike modes;
- trace a bundle of parallel rays from the aperture through the main reflector and the (not yet known subreflector) to the feed;
- determine the subreflector profile from the above procedure such that all rays intersect the same point in the feed phase centre.

The expansion in Zernike modes is convenient because this is the mode representation being used to shape the reflector system in the first place, and because these modes are also used in the mechanical analysis of the thermal distortions. In principle, the determination of the subreflector profile could be done using any representation for the reflectors.

The procedure has been followed for a number of thermal cases as well as for gravitational distortion and the results, presented as radiation pattern for the distorted main reflector with the appropriate correcting subreflector, are shown in Figure 4 in the narrow plane and in Figure 5 for the broad plane.

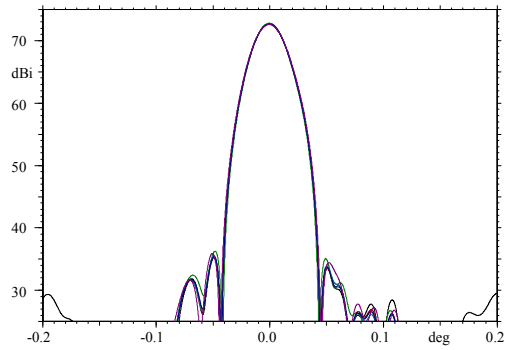

Figure 4. Narrow plane, correcting subreflector.

The plots contain many curves, including the nominal pattern, and is a strong indication that the compensating effect of the subreflector is highly successful.

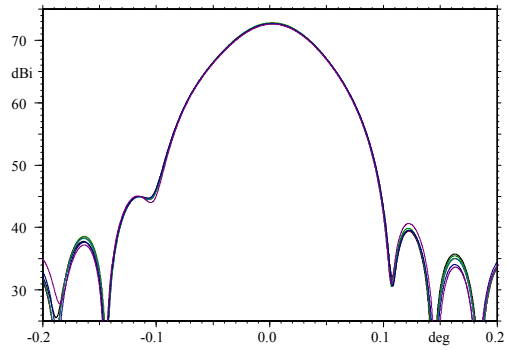

Figure 5. Broad plane, correcting subreflector.

The required subreflector profiles are of course not the same for all thermal scenarios, which is why in practice it will be necessary to have a dynamically controllable surface. A further description of such system is given in the following paragraph.

Deformable, electroformed Nickel reflector technology

The conformable reflector is based on a Nickel shell obtained by replication from a master by means of galvanic electroforming. The process was developed by Media Lario in the middle of the nineties for the production of the XMM-Newton mission mirror modules, each of them consisting of 58 nested high-

accuracy mirror shells specifically designed for collecting low energy X-rays. The process is suitable to replicate all kind of surfaces like mirrors and reflectors, as well as closed shells for X-ray applications. In this respect Media Lario has tuned the production of opens surfaces producing the reflector panels for the European prototype of the ALMA (Atacama Large Millimetre Array) radio telescope.

The technology has already been demonstrated to achieve an rms accuracy of the order of 1 μm for reflectors of 200 – 300 mm in diameter. In addition the high degree of flexibility on the thickness and the diameter of the metal shell together with low recurrent production cost make the Nickel electroforming process particularly suited to the development of a conformable subreflector. Indeed the main point in the design and development of a conformable reflector is the reflective thin shell that must allow the required deformation with reasonable forces and enough stiffness at the same time.

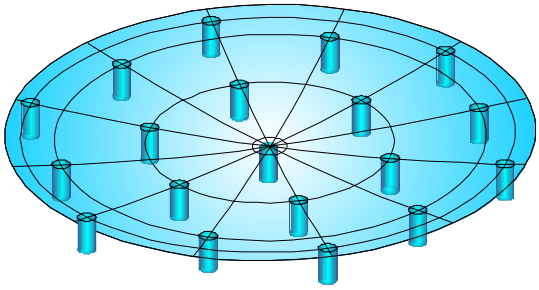

Figure 6. Concept of the conformable concave subreflector with the position of the 19 actuators.

The design of the conformable subreflector is based on the concept shown in Figure 6. A uniform spherical concave Nickel shell with a diameter of 162 mm and a radius of curvature of 1.2 m, is suspended on 19 linear actuators The design of the system has included the optimisation of a few key parameters that strongly affect the structural behaviour of the subreflector. In particular the thickness of the Nickel shell, the number and position of the actuators and the details of their mechanical interface to the reflector are related both to the shape correction that the conformable subreflector has to implement and to the required accuracy and forces. As an example, Figure 7 shows the analysed behaviour of the surface rms accuracy and the maximum actuator force for a given correction shape as a function of the reflector thickness for the above mentioned actuator configuration. A trade off is thus necessary to improve the accuracy from one side and to avoid too large forces on the other. The analyses performed on the target deformation shapes have suggested a reflector thickness of 0.5 mm.

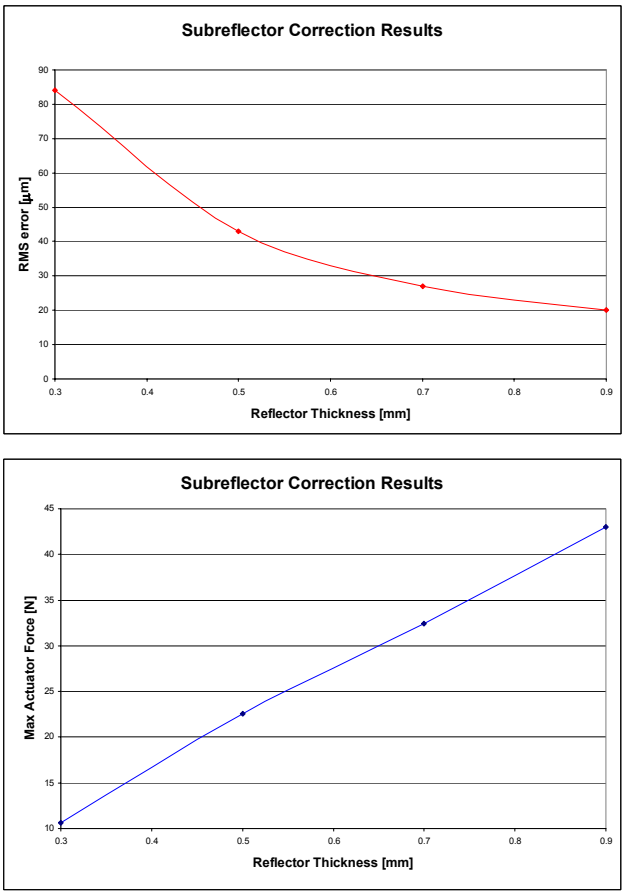

Figure 7. Rms accuracy and maximum actuator force as a function of the reflector thickness.

The accuracy of the correction can be improved by a proper design of the interfaces between the reflector and actuators. Indeed a local increase of the shell stiffness distributes the displacement of each actuator on a larger area, improving the rms accuracy up to about 30%. Again an optimisation analysis has been done to identify the best geometrical solution, resulting in a 0.2 mm thick, 15 mm diameter interface pad between the reflector and each actuator. In the developed prototype the interfaces have just been glued on the back of the reflector but more sophisticated designs are possible, exploiting the possibility offered by the electroforming technology of selectively manufacturing shells of variable thickness.

For ground application the impact of gravity on the achievable accuracy must be taken into account, with particular attention to the case of thin metal shell. The gravity contribution has been analysed by simulating the correction of the very first non-trivial Zernike modes, i.e. defocus and astigmatism. The residual deformation after correction along a radial cross section of the reflector is shown in Figure 8 for the defocus case and for different values of the shell thickness. The peak error before correction at the reflector edge was 10 μm. The strong impact of gravity is evident in the case of the thinnest shell. Nevertheless to a first order

approximation the contribution of gravity is independent from the value of the error to be corrected, so it is expected that gravity can be neglected for large corrections, greater than 100 μm. The rms value of the residual deformation is about 1 μm for the defocus case with 0.5 mm thick shell. As expected the corresponding value for the correction of the astigmatic error is lower, about 0.4 μm.

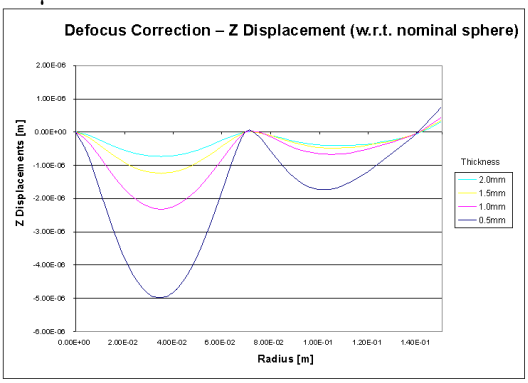

Figure 8. Residual deformation after correction of defocus error in presence of to gravity. The deformation is represented along a radial section of the reflector for different thickness.

Experimental model

The conformable reflector prototype is shown in Figure 9. It should be noted that the main interest in the design and development of the prototype was addressed to the reflector itself and to its mechanical and radio frequency performances. The design of the support structure has been optimised and the chosen actuators are standard off-the-shelf components. As a result the overall system appears unnecessarily cumbersome and bulky.

As already mentioned the reflector is a 0.5 mm thick uniform spherical concave Nickel shell with a diameter of 162 mm and a radius of curvature of 1.2 m. The spherical shape has been chosen to simplify the master manufacturing; much more complicated surfaces can be replicated without difficulties, provided a master is available. The front surface of the reflector is gold covered in the present design. A wide range of other surface treatments are possible if necessary.

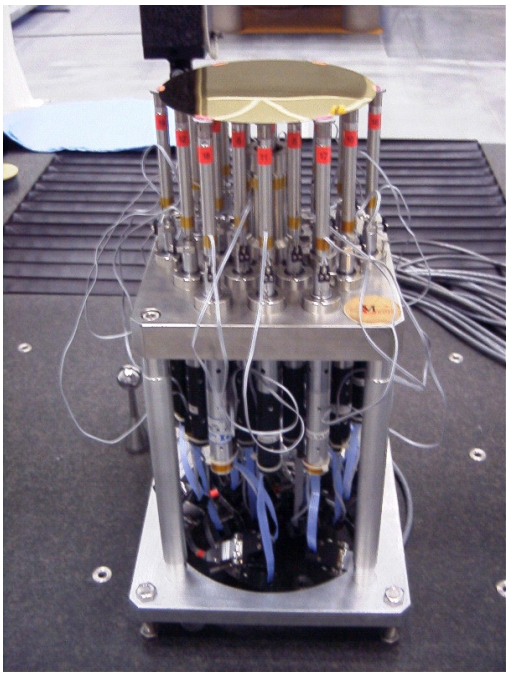

Figure 9. Conformable subreflector prototype.

The reflector is suspended by 19 linear actuators in a hexagonal grid. It should be noted that the edge of the metal shell is completely free and that there is no constraint on the shell except for the attachment points to the actuators. An external rim would have reinforced the reflector edge improving the achievable accuracy but resulting in unacceptable high forces. As mentioned the actuators are standard off-the shelf components consisting of a DC-motor, a gear stage and an optical incremental encoder with a nominal accuracy of 0.1 μm.

Each actuator is driven in closed loop by a distributed control system supervised by computer-based software. The actual displacement of each actuator, and consequently of the reflector at the actuator position, is monitored by the encoder through which the control loop is closed. Although such solution is simple and easy to implement, the lack of a direct real time absolute measurement of the reflector shape is the main source of error in the reflector positioning. Indeed it is not possible to account for the mechanical play of the actuators and of all the mechanical interfaces up to the reflector.

The maximum expected axial force required by each actuator to implement the target deformations is of the order of 30 N for both traction and compression. The transmission of the force to the reflector must avoid any constraints to the reflector tip, tilt and small transversal displacement. Such result has been obtained through a magnetic joint, which has also the advantage to keep the rotation point as close to the reflector surface as possible. Each joint consists in the ferromagnetic interface pad described above and glued on the back of

the reflector and a custom designed magnet screwed on the actuator extension strut.

The target deformations are, as already explained, derived for a realistic scenario for the ADMIRALS antenna [3]. Four thermal load cases simulating the environment of a 600 km polar orbiting spacecraft plus a 9.81 m/s^2 specific gravity load have been applied, by Finite Element Analysis (FEA), to the antenna main reflector assuming a very simple design based on a 20 mm thick honeycomb structure covered by two 0.6 mm thick electroformed Nickel shell. The thermal load cases included uniform hot (+85 °C) and cold (–22.5 °C) temperature changes, a thermal gradient of 3 °C through the main reflector thickness and a thermal gradient of 20 °C along the main reflector long axis.

The impact on the pattern was shown in Figures 2 and 3, while the theoretical improvement by using a reconformable subreflector was shown in Figures 4 and 5. The required deformations are now applied to the experimental model to investigate to which extent they can be reproduced in practice.

An example of the target deformation is shown in Figure 10 for the cold load case in which the peak-to-peak displacement is of the order of 1 mm. The displacement is even larger for the load case corresponding to a thermal gradient through the reflector thickness.

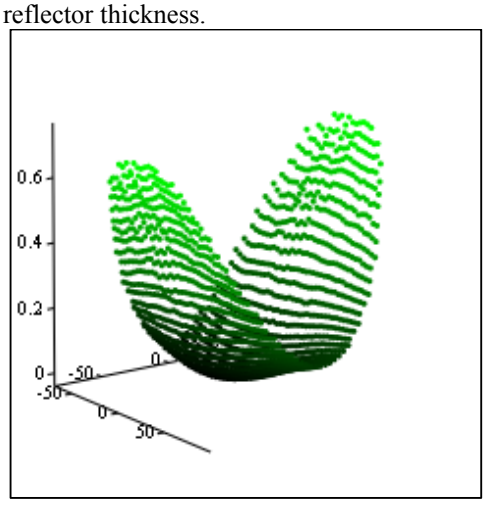

Figure 10. Target deformation of the subreflector for the cold load case (+85 °C). Dimension in millimeters; not to scale.

During the experimental verification, the subreflector surface has been measured on a 10 mm square grid by means of a 3-dimensional contact metrology equipment capable of an absolute accuracy better than 1 μm rms. Table 1 resumes the mechanical performance of the conformable subreflector for the five tested target shapes and compares the experimental results with the numerical prediction of the analysis. The worst performances correspond to the more demanding load cases in terms of peak-to-peak displacement. In all cases the rms accuracy is better than 17 μm. The residual error for the cold load case and the corresponding Zernike mode decomposition of the rms error up to the 28th mode are shown in Figure 11. The first mode is piston whereas the 2nd and 3rd modes are tip and tilt. The 4th mode is responsible for a defocus error that together with the 14th mode (*ashtray* mode) are the two main contributions to the rms inaccuracy at low mode order. The remaining contribution to the overall rms error comes from modes of order higher than the 19th that cannot be obviously corrected by the 19 actuators of the conformable reflector.

Load Case	Numerical	Experimental
+85 °C	13.4 μm	17.1 μm
–22.5 °C	5.8 μm	7.34 μm
3 °C gradient	16.5 μm	15.3 μm
20 °C gradient	8.5 μm	6.8 μm
Gravity	4.3 μm	4.8 μm

Table 1. Numerical and experimental performance of the conformable subreflector in terms of surface rms accuracy.

During the experimental phase the linearity and the repeatability of the prototype have been also checked. It has been verified that scaling the actuator displacement by an arbitrary factor, gives indeed a deformed surface which represents the target shape scaled by the same factor, within an rms error always smaller than the full displacement error. Also excellent repeatability has been demonstrated for the rms error whereas the average reflector position tend to slowly drift after repeated back and forward displacement mainly due to the actuator backlash.

Determining the optimum actuator position

From a mechanical point of view the target of the conformable reflector is to reproduce with the highest possible accuracy the target surface required to meet the desired radio frequency performance. The simplest approach consists in just moving the actuators to the nominal target positions but in general this is not the configuration that gives the highest accuracy or lower rms error.

In addition the a priori estimation of the required forces and the achievable rms error for a given target deformation require the application of a mechanical Finite Element Analysis software. Clearly in an actual field application, both on ground and in space, a much more efficient and fast approach is required to get such information in real time.

To solve both problems a best fitting approach has been developed based on a standard Least Square fitting of actuator influence functions that can be easily implemented on a real time system. The method consists in calculating by Finite Element Analysis the reflector deformations when a unit force is applied to just one actuator at time, and then to determine the best linear superposition that minimise the rms error between such superposition and the target shape.

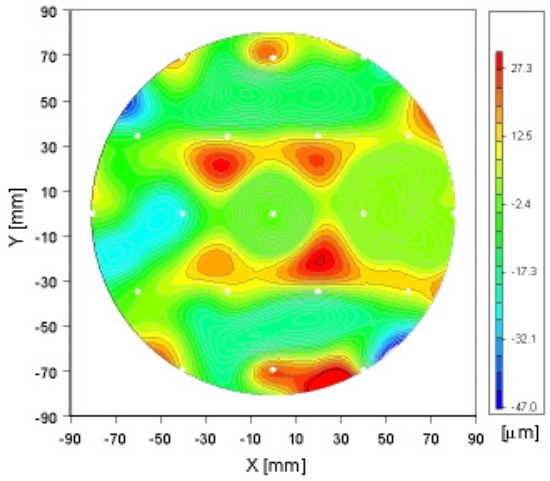

(a)

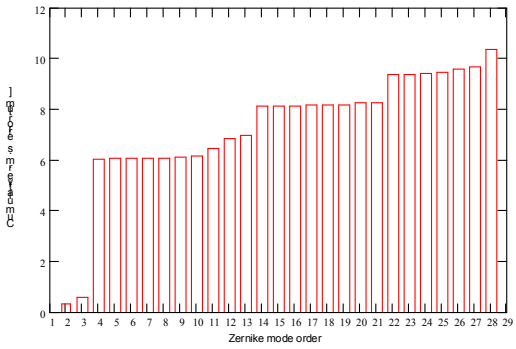

(b)

Figure 11. (a) Residual error for the cold load case (+85 °C); The white dots represent the actuator position. (b) Cumulative Zernike mode decomposition of the rms error.

The only complications here arise from the fact that the single actuator influence function can not be calculated by Finite Element Analysis since the condition for global equilibrium to vertical translation and to tip and tilt rotations would not be satisfied. In addition the actuators used in the development of the prototype are displacement actuator and not force actuator.

The fitting procedure here starts with the definition of 16 independent sets of forces, each of them satisfying the equilibrium conditions. Then the corresponding 16 influence functions are calculated by Finite Element Analysis and linearly superimposed to the three rigid modes (tip, tilt and piston) for a total of 19 modes. The superposition force coefficients are then calculated by Least Square Method allowing the determination of the optimum actuator position, the required forces and the highest achievable accuracy.

The application of the method to the analysed load cases has shown a theoretical improvement of about the 20% in the rms error, corresponding, by the Ruze relation, to a reduction of about 40% in the peak loss of the antenna gain between the nominal and the actual radiation pattern.

In principle the best fitting approach can be further extended to include, as an adjustable parameter, also the angle between the actuator grid and the deformed shaped that must be reproduced, thus allowing the control of an additional degree of freedom

RF performance of measured subreflector profiles

The measured surface data consist of corresponding (x,y,z)-coordinates for points on the experimental model of the subreflector. These data are imported into the reflector analysis program GRASP8 [6]. This program is very general and can predict the radiation pattern from numerous reflector antenna systems, including shaped reflectors with surface distortions superimposed. In the present case we combine the measured subreflector profile with the thermally (or gravitationally) distorted main reflector, and perform a radiation-pattern analysis to see how well the original pattern is recovered.

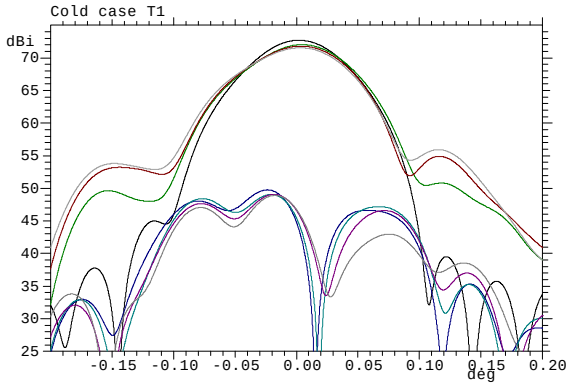

(a)

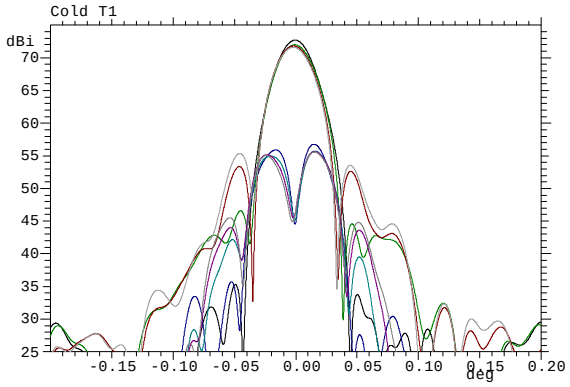

(b)

Figure 12 Nominal, predicted and measured pattern restoration for a cold thermal load case. (a) broad pattern plane, (b) narrow pattern plane.

The results are shown as both co- and cross polar patterns for a cold load case (which is the worst of all the cases considered) in Figure 12. The figures contain many curves that may not be easily distinguishable, so some explanation is in order.

First, there are the nominal data that are identical to the nominal curves in Figures 2 and 3. Next, there are results for a deformed main reflector with predicted (Finite Element Analysis) data for the experimental model. Finally, there are data for the deformed main reflector and the measured subreflector. The most important findings are the following.

- The compensating subreflector improves the radiation pattern significantly, but results in slightly lower peak gain and increased sidelobes.
- There is excellent agreement between the measured and predicted mechanical deformations on the subreflector.
- The cross polar pattern is not degraded by the same amount as the copolar pattern.

The antenna community has in general a high degree of confidence in the pattern prediction of reflector antennas of general shape and it is expected that RF measurement of the antenna configuration with a distorted main reflector and a compensating subreflector will lead to the same conclusions that can be drawn from the above results. It should be noted that such measurements would be extremely complicated to carry out, and require RF measurements in a thermal chamber.

Conclusions

The work has shown that it is possible to compensate errors on a main reflector by modifying the subreflector shape. Such compensation requires a deformable subreflector, which has been implemented in electroformed Nickel technology. The technology is applicable to millimetre wave antennas with distortions that are typically induced by the thermal loads experienced on a spacecraft. For larger deformations such as those required in beam contouring, further developments are needed in the area of surface technology.

A particularly important aspect is the ability to dynamically change the subreflector shape, an essential feature if the technique shall be applied to millimetre or sub-millimetre sounders on geostationary spacecraft. It will be necessary to make a decision if the subreflector shape can be determined from models of the main reflector distortion, or from instruments or sensors on the spacecraft that constantly monitors the status of the reflector.

References

[1] A. Greve, J.W.M. Baars, J. Penalver, B. LeFloch, "Near-Focus Active Optics: An Inexpensive Method to Improve Millimetre-Wavelength Radio Telescopes", Radio Science, Vol 31, No 5, 1996.

[2] H. H. Viskum, K. Pontoppidan, G. Crone, P.J.B. Clarricoats, “Coverage Flexibility by Means of a Reconformable Subreflector”, IEEE APS Symposium 1997, pp.1378 – 1381.

[3] “Antenna Development in Millimetre/ Submillimetre-wave Range for Astronomy and Limb Sounding – ADMIRALS”, ESA Contract13669-Astrium.

[4] Jørgensen, R., Padovan, G., de Maagt, P. Lamarre, D. & Costes, L., ”A 5-Frequency Millimetre Wave Antenna for a Spaceborne Limb Sounding Instrument”, IEEE Transactions on Antennas and Propagation, Vol. 49, No. 5, pp. 703-714, May 2001.

[5] Viskum, H.-H., “Manual for DORELA – Dual Offset Reflector with Elliptical Aperture”, TICRA Report S-529-02, 1991.

[6] Pontoppidan, K. (Ed.), “Technical Description of GRASP8”, TICRA Report, February 2003. (Available as part of the free, downloadable student edition of GRASP8 from www.ticra.com).